Scorpion-inspired flank surface texturing for biomimetic reduction of frictional heating and wear in dry turning

Deepak K. Pandey
Designing Alley (Part of Anirveda Engineering Pvt Ltd),
Shriram Institute for Industrial Research, Civil Lines,
New Delhi-110016, India
Email: pdk201994@gmail.com

Abstract

Natural arthropod cuticles exhibit micro-scale surface features that reduce drag and control interfacial interactions during motion. The cuticle of desert scorpions exhibits periodic ridge–groove microstructures that regulate contact and reduce resistance during locomotion over solid terrains. Inspired by the micro-topography of scorpion skin, this study translates a biological surface concept into a functional engineering solution for tribological control in dry machining. Bioinspired micro-grooves with 0.2 mm spacing were fabricated on the flank surface of tungsten carbide inserts using Nd:YAG laser texturing. A comparative experimental investigation between conventional and textured inserts was conducted during dry turning of C-20 steel over a wide range of spindle speeds, feed rates, and depths of cut. Tool performance was quantified through tool-tip temperature rise, insert wear by weight loss, SEM wear morphology, and 3D surface profilometry of the machined workpiece. The biomimetic textured inserts exhibited a 1–6 °C reduction in temperature rise, up to 50% reduction in wear, corresponding to nearly 100% improvement in effective tool life, along with significantly improved surface finish at higher machining parameters. The improvements are attributed to reduced real contact area, suppression of adhesive junction formation, and debris entrapment, mechanisms analogous to drag-reduction strategies observed in scorpion cuticle morphology. The study demonstrates how bioinspired surface architecture can be functionally transferred to cutting tools to achieve measurable tribological and thermal benefits in a practical engineering process.

Keywords: Biomimetic surface; Scorpion skin; Tribology; Dry machining; Flank wear

1. Introduction

Machining operations constitute a major share of industrial energy consumption, and a significant portion of this energy is dissipated as frictional heat at the tool–chip and tool–workpiece interfaces [1–3]. This friction accelerates tool wear, elevates cutting temperature, degrades surface finish, and limits the feasibility of dry machining [4]. With growing emphasis on sustainable and green manufacturing, minimizing friction and wear in machining processes without the use of coolant has become an important research objective [5–8].

Surface texturing has emerged as an effective technique to control tribological behavior by modifying the real area of contact between interacting surfaces. Micro- and nano-scale textures such as grooves, dimples, and cross-hatches can trap wear debris, reduce adhesive contact, and alter local stress distribution at the interface [9–12]. Among the available techniques, Laser Surface Texturing (LST) has gained particular importance because it allows precise and repeatable fabrication of micro-features on hard tool materials such as tungsten carbide without affecting their bulk properties [13,14]. In machining applications, texturing has been predominantly applied on the rake face of cutting tools to influence chip flow and reduce adhesion [12,15,16]. However, recent investigations indicate that the flank face also plays a crucial tribological role because it remains in continuous contact with the newly machined surface and contributes significantly to frictional heat generation and flank wear [11,16,17]. Therefore, flank face texturing has been proposed as an effective approach to reduce friction at the tool–workpiece interface during dry turning.

Bio-inspired surface textures derived from natural organisms such as shark skin, reptile scales, lotus leaves [18], and scorpion skin have gained significant attention in tribology because of their inherent drag-reducing, anti-adhesive, and wear-resistant characteristics developed through evolutionary optimization [14,19–22]. The micro-topography of scorpion cuticle consists of longitudinal ridges and grooves that are known to regulate interfacial interaction during locomotion by reducing drag and controlling contact with surrounding surfaces [23]. SEM observations reported by Han et al. [21] show that these ridges are periodically spaced and act to interrupt continuous contact, thereby minimizing resistance during motion over granular and solid terrains. This natural strategy of contact regulation and drag reduction provides a functional template for engineering surfaces where sliding interaction governs frictional losses. These natural surfaces possess micro- and nano-scale patterns that effectively control interfacial interactions, enabling reduced resistance, efficient motion, and self-cleaning behavior. When such textures are replicated on engineering surfaces, particularly on cutting tools through laser surface texturing, they have been shown to significantly modify contact mechanics at the tool–chip and tool–workpiece interfaces [16,17,22,24]. The micro-grooves and patterned features reduce the real area of contact, thereby minimizing adhesive bonding and suppressing built-up edge formation. Additionally, the grooves act as micro-reservoirs that trap wear debris, reducing third-body abrasion and stabilizing sliding conditions. The altered surface topography also redistributes local contact stresses and lowers

interfacial pressure, further decreasing adhesion and wear. A direct consequence of these combined mechanisms is a reduction in frictional heat generation, leading to lower interface temperature, improved tool life, and better surface integrity of the machined component. Importantly, this approach enhances machining performance through passive geometric modification rather than external lubrication, making bio-inspired textures particularly suitable for dry and sustainable machining environments [7,9,25,26].

Despite the encouraging results reported in the literature, most studies focus on limited combinations of texture geometry and machining parameters. There remains a lack of systematic studies that combine (i) realistic industrial insert geometries, (ii) bio-inspired flank texturing, and (iii) a wide range of machining parameters such as spindle speed, feed rate, and depth of cut under dry conditions [22,27,28]. Furthermore, several studies report reduction in tool temperature without clearly distinguishing whether this reduction arises from enhanced cooling or from reduced frictional heat generation at the interface. In the present work, this biological surface strategy is translated to the flank face of a cutting insert, where continuous sliding contact with the machined surface governs frictional heat generation and wear. By replicating the ridge–groove concept observed in scorpion cuticle, the study investigates whether biomimetic surface architecture can measurably alter tribological behavior in a real machining process.

2. Materials, Tool Geometry and Laser Surface Texturing

The surface texture implemented in this study is not an arbitrary groove pattern but is derived from the micro-scale morphology observed on scorpion cuticle, which is known to reduce drag during locomotion. The intent is to replicate this biological strategy on the flank face of a cutting tool, where continuous sliding contact governs frictional heat generation and wear. This section describes the materials used in the study, the geometric configuration of the cutting insert and workpiece, and the laser surface texturing process employed to reproduce the scorpion-inspired micro-grooves on the tool insert.

2.1. Tool Insert and Workpiece Material

Tungsten carbide (WC–Co) inserts were selected for the present investigation because of their widespread use in industrial turning operations, high hardness, superior wear resistance, and excellent thermal stability under dry cutting conditions. The inserts employed in this study were uncoated and equilateral triangular in shape with internal angles of 60°, a side length of 1.5 cm, and a thickness of 0.5 cm. This geometry is representative of standard single-point cutting inserts commonly used in lathe machining. The workpiece material used for the experiments was C-20 medium carbon steel in cylindrical rod form. C-20 steel is widely used in shafts, automotive components, and general

engineering applications due to its good machinability and balanced mechanical properties, making it suitable for evaluating practical machining performance. The chemical compositions of both the tungsten carbide insert and the C-20 steel workpiece are provided in Table 1.

Table 1. Chemical composition of tungsten carbide insert and C-20 steel workpiece.

	Elements	Wt.%
Tool Insert (Cutting tool)	Tungsten Carbide	84.96
	Cobalt	14.98
	Iron	0.048
WorkPiece	Iron	99.101
	Carbon	0.200
	Manganese	0.465
	Phosphorus	0.024
	Sulphur	0.024
	Silicon	0.186

The dimensional representation of the insert, the inspiration from scorpion skin, and the textured flank region are illustrated in Figure 1.

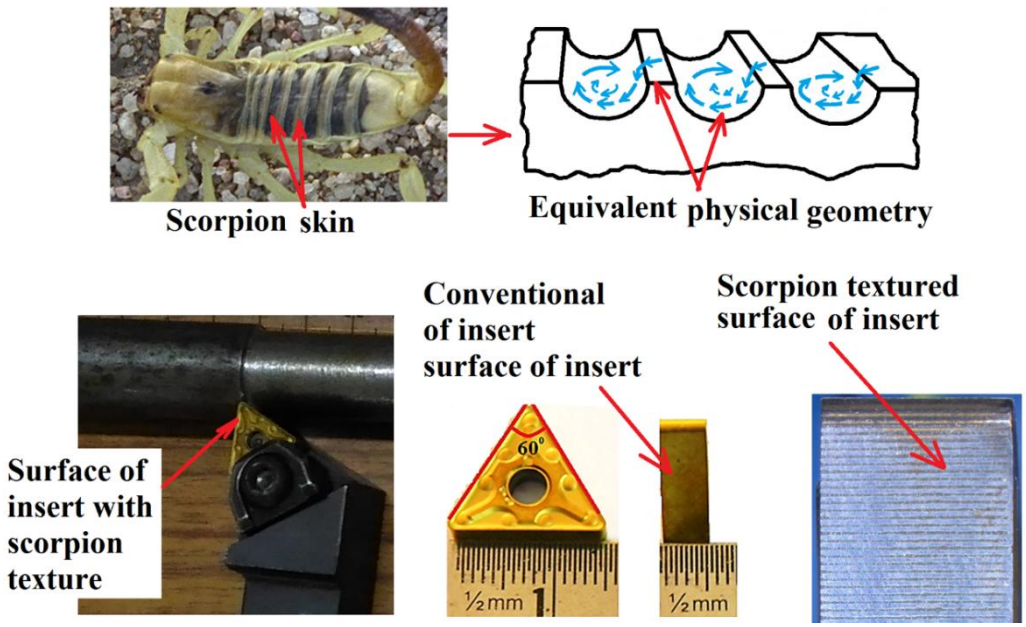

Figure 1: Scorpion cuticle morphology and its equivalent micro-groove model used for flank biomimetic surface texturing: (top) scorpion skin showing ridge–groove structure; (bottom left) insert mounted on tool holder; (bottom center) conventional triangular insert surface; (bottom right) laser-textured flank surface with 0.2 mm groove spacing.

2.2. Geometric Features of the Tool Insert

The triangular insert provides three identical cutting edges, of which one edge is actively involved in machining at a time. During turning, while the cutting edge shears the material, the flank surface of the

insert remains in continuous sliding contact with the newly machined surface of the workpiece. This continuous contact generates significant frictional heat and is primarily responsible for flank wear under dry machining conditions. Since the flank face plays a dominant role in tool–workpiece frictional interaction, it was selected as the region for biomimetic surface texturing. Modifying the surface characteristics of this region is expected to reduce real contact area, minimize adhesion, and consequently reduce frictional heat generation and wear.

2.3. Laser Surface Texturing Inspired by Scorpion Skin

Bio-inspired micro-grooves were fabricated on the flank surface of the tungsten carbide inserts using a fiber laser system based on Nd:YAG crystal with a wavelength of 1064 nm. The texture pattern was inspired by the micro-features observed on scorpion skin, which are known to reduce drag and resistance during motion. Uniform grooves with a spacing of 0.2 mm were produced along the flank surface. The groove spacing of 0.2 mm was selected to be of the same order of magnitude as the ridge spacing reported in scorpion cuticle morphology [21], ensuring that the engineered texture retains geometric similarity with the biological prototype. The laser parameters employed during the texturing process are listed in Table 2.

Table 2. Laser processing parameters used for fabrication of scorpion-inspired micro-grooves on the flank surface

S. No.	LASER Parameters	Values
1.	Crystal used for LASER	Nd: YAG
2.	Laser Power (W)	20
3.	Wavelength (nm)	1064
4.	Pulse Frequency (kHz)	2
5.	Distance between two grooves (mm)	0.2
6.	Scanning speed (mm/s)	5

During laser ablation, debris and recast material are often deposited around the grooves. To remove these irregularities and obtain clean groove geometry, the inserts were subjected to a lapping process after texturing. The effectiveness of this process was verified using scanning electron microscopy. SEM images of the textured insert before and after lapping are shown in Figure 2(a) and 2(b), respectively.

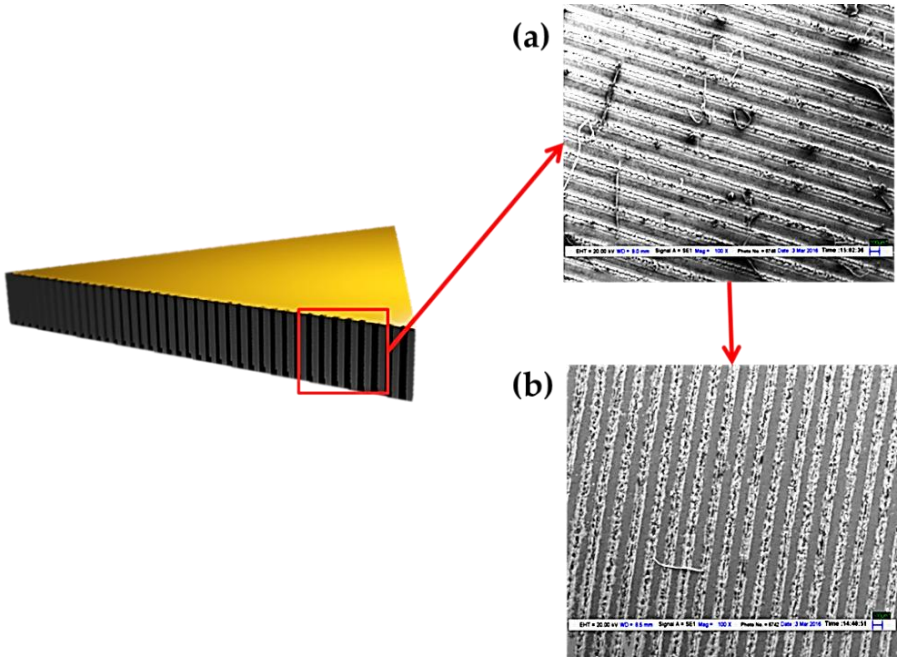

Figure 2: SEM images of laser-textured flank surface: (a) after laser texturing without lapping; (b) after lapping showing clean and well-defined grooves.

2.4. Experimental Setup and Machining Parameters

Turning experiments were conducted on a Pioneer GHL-175 semi-automatic lathe machine. The experimental setup for performing turning operations using the single-point cutting tool is shown in Figure 3.

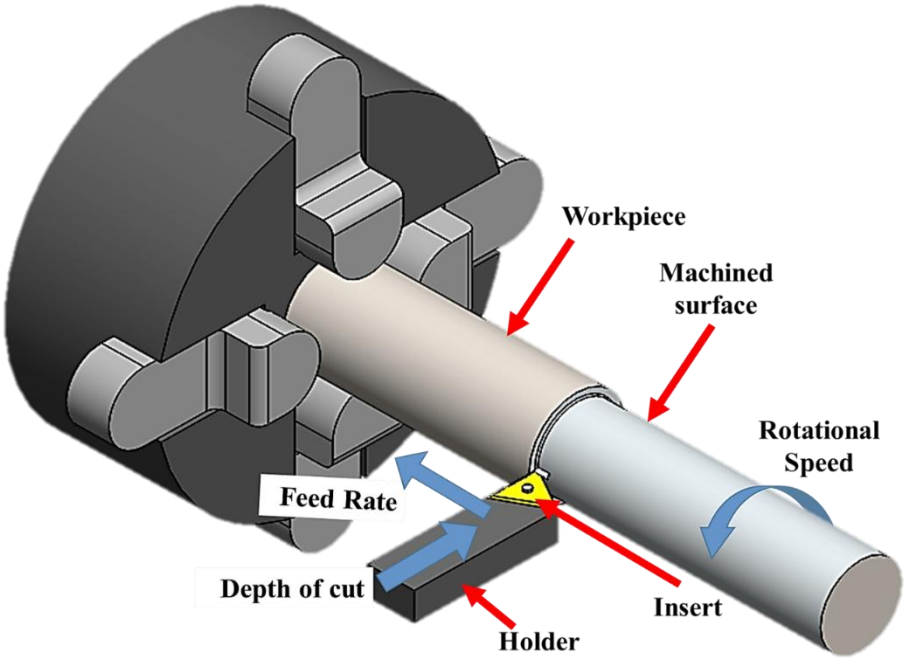

Figure 3: Experimental setup for dry turning of C-20 steel using a single-point tungsten carbide insert on a semi-automatic lathe.

The relative positioning of the conventional and textured inserts with respect to the workpiece and the direction of tool motion during turning are illustrated in Figure 4.

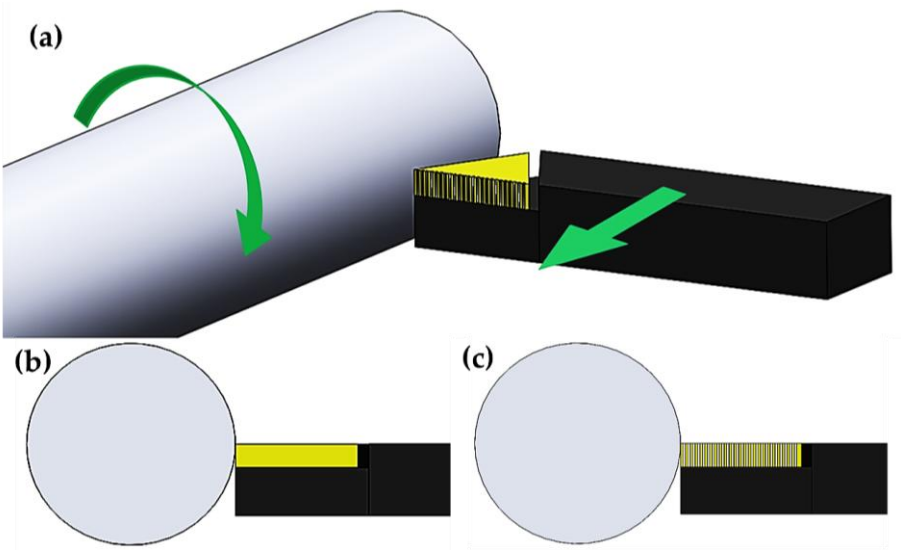

Figure 4: Relative positioning of tool insert and workpiece during turning: (a) direction of tool motion; (b) conventional insert in contact with workpiece; (c) textured insert showing flank interaction region.

The machining parameters selected for the experiments are provided in Table 3. Each experiment consisted of a cutting length of 12.5 cm repeated for 15 passes under dry machining conditions.

Table 3. Machining parameters selected for dry turning experiments

Parameters	**Values**		
Spindle Speed (rpm)	315	500	775
Depth of cut (mm)	0.12	0.16	0.20
Feed rate (mm/rev)	0.4	0.8	1.6
Cutting length	12.5 (cm) x 15 passes		
Machining condition	Dry		

2.5. Wear Quantification and Percentage Reduction Calculation

The wear of the cutting inserts was quantified by measuring the weight loss before and after each machining trial using a precision electronic balance. The initial weight of each insert was recorded prior to machining, and the final weight was measured after completion of the turning operation for a given parameter set. The difference between the initial and final weight represents the material removed from the insert due to wear. To compare the performance of conventional and textured inserts under identical machining conditions, the percentage reduction in wear for the textured insert was calculated using:

$$\%\ Wear\ Reduction = \frac{W_c - W_t}{W_c} \times 100 \quad (1)$$

where Wc is the weight loss of the conventional insert and Wt is the weight loss of the textured insert for the same spindle speed, feed rate, and depth of cut.

The maximum percentage reduction reported in this study corresponds to the machining condition where the difference between the two inserts was highest.

2.6. Estimation of Tool Life Using Wear Data and Tool Life Relation

In turning operations, tool life is primarily governed by progressive flank wear. Although the present study did not directly measure tool life in terms of machining time to reach a specified wear limit, the relative tool life of the inserts can be estimated from the measured wear data using the fundamental tool life relationship. According to Taylor's tool life equation:

$$V\,T^n = C \quad (2)$$

where $V$is the cutting velocity, $T$is the tool life, n is the tool wear exponent, and $C$is a constant for a given tool–workpiece combination. For identical machining conditions, the cutting velocity Vremains constant for both conventional and textured inserts. Hence, tool life becomes inversely related to the rate of wear progression at the flank surface.

Since both inserts were operated for the same machining duration, the weight loss measured from each insert represents the amount of material removed due to flank wear over equal time. Therefore, wear is inversely proportional to tool life, and the ratio of tool life of the textured insert to that of the conventional insert can be estimated as:

$$\frac{T_t}{T_c} = \frac{W_c}{W_t} \quad (3)$$

where $T_t$and $T_c$are the tool lives of textured and conventional inserts, respectively, and W_c and $W_t$are their corresponding weight losses under the same machining condition.

The percentage improvement in tool life is then calculated using:

$$\%\ \text{Tool life improvement} = \left(\frac{W_c}{W_t} - 1\right) \times 100 \quad (4)$$

For the machining condition where the maximum difference in wear was observed, the textured insert exhibited nearly twice the effective tool life compared to the conventional insert. This substantial increase in tool life confirms that the scorpion-inspired ridge–groove structure slows down wear

progression by reducing adhesion, trapping debris, and lowering frictional interaction at the flank interface.

Thus, the wear measurements not only quantify material loss but also provide a reliable estimation of tool life improvement achieved through biomimetic flank surface texturing under dry machining conditions.

2.7. Experimental Procedure

The experimental study was carried out in a systematic manner to ensure repeatability and accuracy of observations. The procedure followed was:

1. Initial dimensions and weight of both conventional and textured inserts were measured.
2. The C-20 steel rod was mounted in the chuck of the lathe machine.
3. The tool holder and insert were fixed on the tool post.
4. Initial temperature at the tip of the insert was measured and recorded.
5. Turning operation was performed by setting the desired spindle speed, feed rate, and depth of cut.
6. The machining operation was repeated for 15 passes for each set of parameters.
7. After machining, the final temperature at the tool tip was recorded.
8. Inserts were re-weighed and measured to determine wear.
9. SEM analysis was carried out to study the wear pattern of the inserts.

3. Results and Discussions

The results presented in this section are interpreted in the context of how the scorpion-inspired surface architecture modifies interfacial tribology at the tool–workpiece interface. Particular emphasis is placed on understanding how the biomimetic groove pattern influences frictional heat generation, wear mechanisms, and surface integrity during sliding contact.

3.1. Effect of Machining Parameters on Tool Tip Temperature (Frictional Heat Generation)

This behavior mirrors the contact-regulation mechanism observed in scorpion cuticles, where ridge structures interrupt continuous surface interaction. The bulk temperature rise measured at the tool tip for both inserts is presented in Figure 5. At lower spindle speed, feed rate, and depth of cut, the temperature difference between conventional and textured inserts is relatively small. However, as machining parameters increase, the conventional insert exhibits a significantly higher temperature rise compared to the textured insert.

This behavior is governed by the physics of frictional heat generation at the flank interface. During turning, the flank surface remains in continuous sliding contact with the newly machined surface.

Increasing spindle speed increases sliding velocity, while higher feed and depth of cut increase the normal load on the flank surface. For the conventional insert, the larger real contact area promotes adhesion and higher interfacial shear stress, which converts mechanical work into heat that is conducted to the tool tip. In contrast, the micro-grooves on the textured insert reduce the real area of contact, interrupt adhesive junction formation, and trap wear debris. As a result, the interfacial shear stress and frictional work are reduced. This leads to a measurable reduction of 1–6°C in temperature rise for the textured insert, particularly at higher machining parameters. The results confirm that the improvement arises from reduced heat generation rather than enhanced cooling..

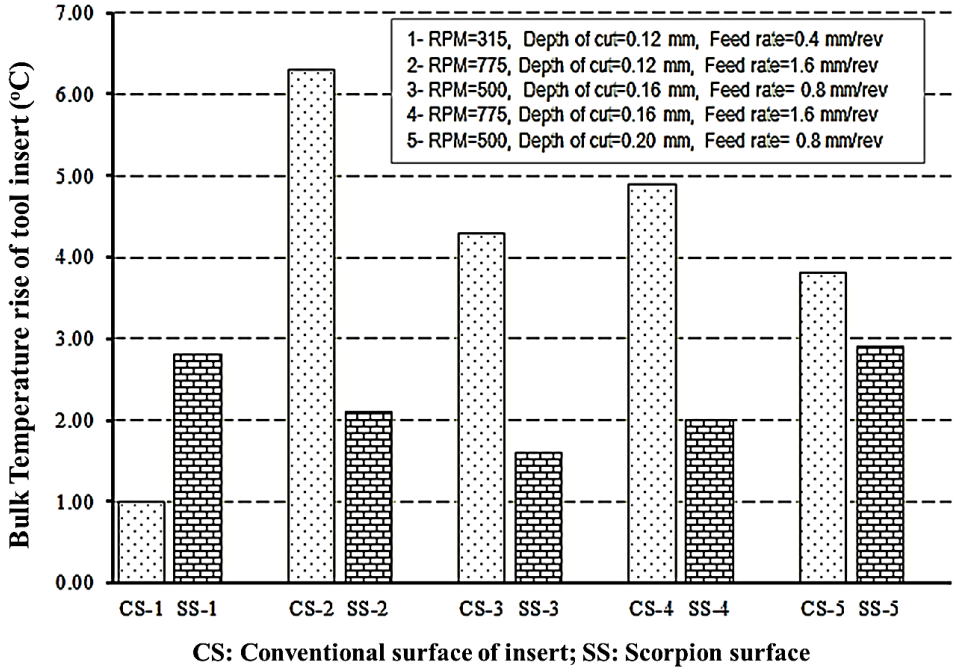

Figure 5: The bulk temperature rise of a tool insert at various parameters

3.2. Wear Analysis Based on Weight Loss of Inserts

The wear behavior of both inserts quantified by weight loss is shown in Figure 6. The conventional insert exhibits significantly higher weight loss across all machining conditions, while the textured insert demonstrates up to 50% reduction in wear, especially at higher spindle speeds and feed rates. Under dry turning conditions, flank wear is dominated by adhesion and abrasion. In the conventional insert, strong adhesive bonding between tool and workpiece leads to material transfer and tearing, while loose debris contributes to third-body abrasion. The grooves in the textured insert act as micro-reservoirs that trap wear particles and reduce abrasive interaction. Simultaneously, the reduced contact area weakens adhesive bonding. This combined effect significantly lowers material removal from the tool surface. The reduced wear of the textured insert directly indicates slower wear progression and therefore longer effective tool life under identical machining conditions.

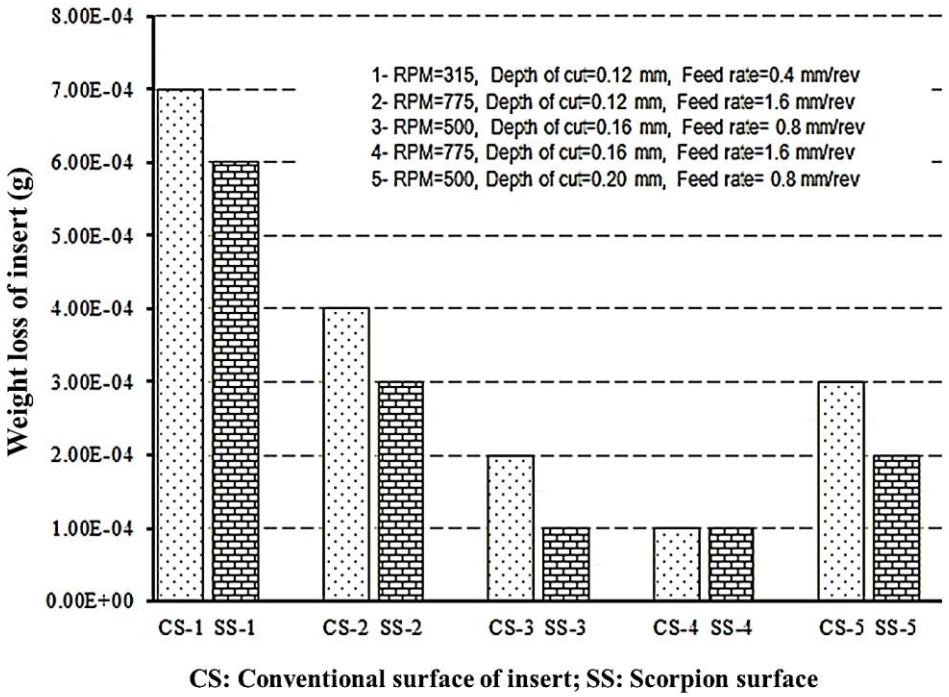

Figure 6: Weight loss of insert (Wear) of tool inserts at various parameters

For the condition at 775 rpm, 0.12 mm depth of cut and 1.6 mm/rev feed, the weight loss of the conventional insert was approximately twice that of the textured insert, leading to 50% wear reduction and nearly 100% improvement in effective tool life as calculated using Eq. (3) and Eq. (4).

3.3. Scanning Electron Microscope (SEM) image for wear pattern

To understand the dominant wear mechanisms operating on the tool inserts under different machining conditions, scanning electron microscopy (SEM) was performed on both conventional and textured inserts after completion of the turning experiments. The SEM micrographs for representative parameter combinations are presented in Figures 7 to 11. These images provide clear visual evidence of how flank texturing alters the nature and severity of wear during dry machining.

Figure 7 corresponds to low machining parameters (315 rpm, 0.12 mm depth of cut, 0.4 mm/rev feed). At this condition, the conventional insert shows the onset of mild abrasive scratches and small regions of adhesive material deposition on the flank surface. These features indicate initial stages of adhesion and abrasion due to sliding contact with the workpiece. In contrast, the textured insert shows very limited signs of wear. The micro-grooves remain clearly visible, and only minor polishing of the groove edges is observed. This suggests that at low loads and speeds, the textured surface effectively reduces continuous contact and prevents the initiation of severe wear.

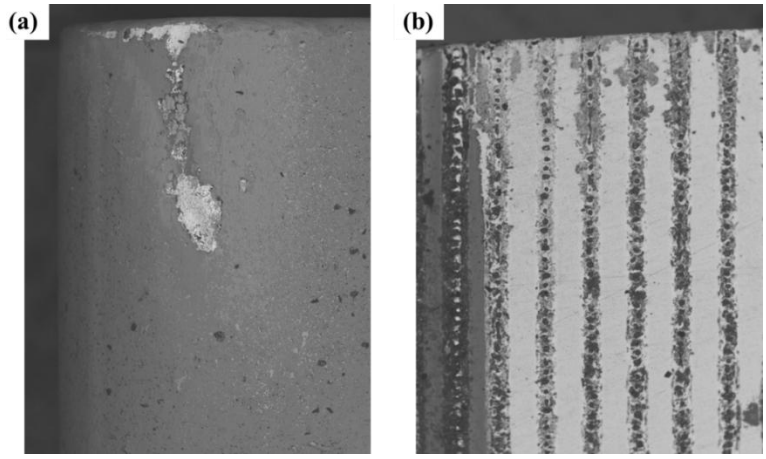

Figure 7: SEM of the (a) conventional and (b) textured tool insert at 315 rpm, depth of cut is 0.12 mm and feed rate is 0.4 mm/rev

Figure 8 represents moderate machining parameters (500 rpm, 0.20 mm depth of cut, 0.8 mm/rev feed). Under these conditions, the conventional insert exhibits pronounced built-up edge formation, deep abrasive grooves, and large regions of adhered workpiece material. The combination of higher normal load and sliding velocity increases adhesive bonding, and the subsequent tearing action produces severe abrasion marks. The textured insert, however, shows comparatively smoother wear tracks. The grooves are still identifiable, and the adhered material is considerably less. The grooves appear to have trapped wear debris, preventing it from ploughing across the surface.

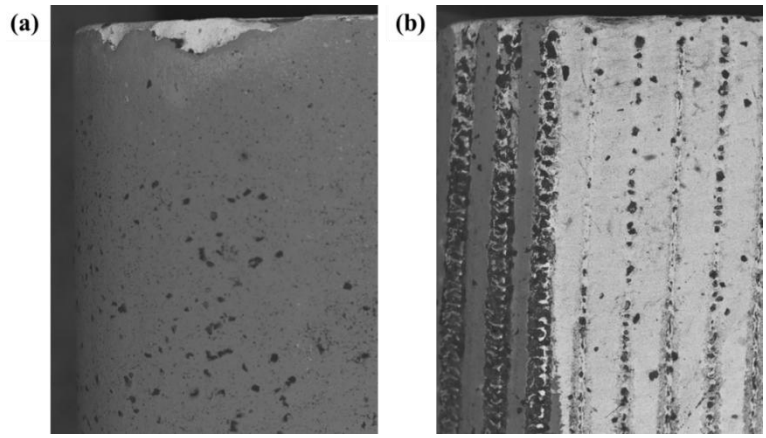

Figure 8: SEM of the conventional and textured tool insert at 500 rpm, depth of cut is 0.20 mm and feed rate is 0.8 mm/rev

Figure 9 shows wear morphology at high spindle speed (775 rpm). The conventional insert surface is heavily smeared with deposited material, indicating strong adhesion and plastic deformation at the flank face. The presence of continuous layers of adhered material confirms severe adhesive wear. In contrast, the textured insert maintains visible groove patterns with limited material deposition. The interruption of contact by the grooves reduces the growth of adhesive junctions even at high sliding speeds.

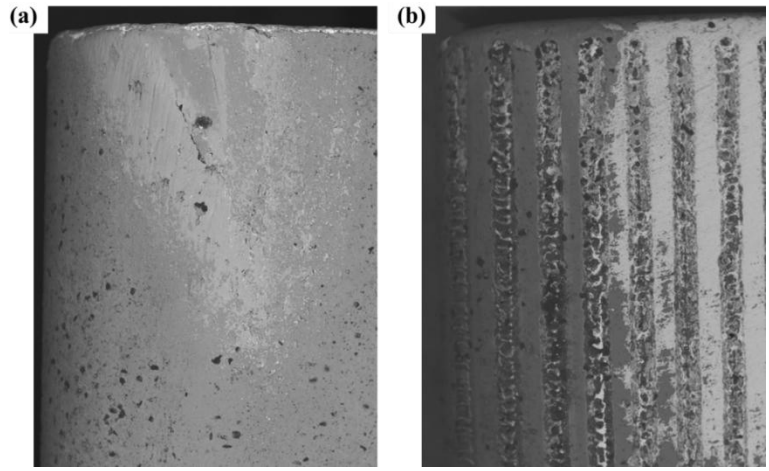

Figure 9: SEM of the conventional and textured tool insert at 775 rpm, depth of cut is 0.12 mm and feed rate is 1.6 mm/rev

Figures 10 and 11 correspond to high feed rate and depth of cut combinations. These conditions generate high contact pressure on the flank surface. The conventional insert shows severe plastic deformation, deep ploughing marks, and extensive adhesion, characteristic of combined adhesive–abrasive wear. For the textured insert, wear appears more uniform and controlled. The groove structure redistributes contact stresses and prevents the development of long continuous wear tracks. Debris particles are observed lodged within the grooves rather than scratching the flank surface.

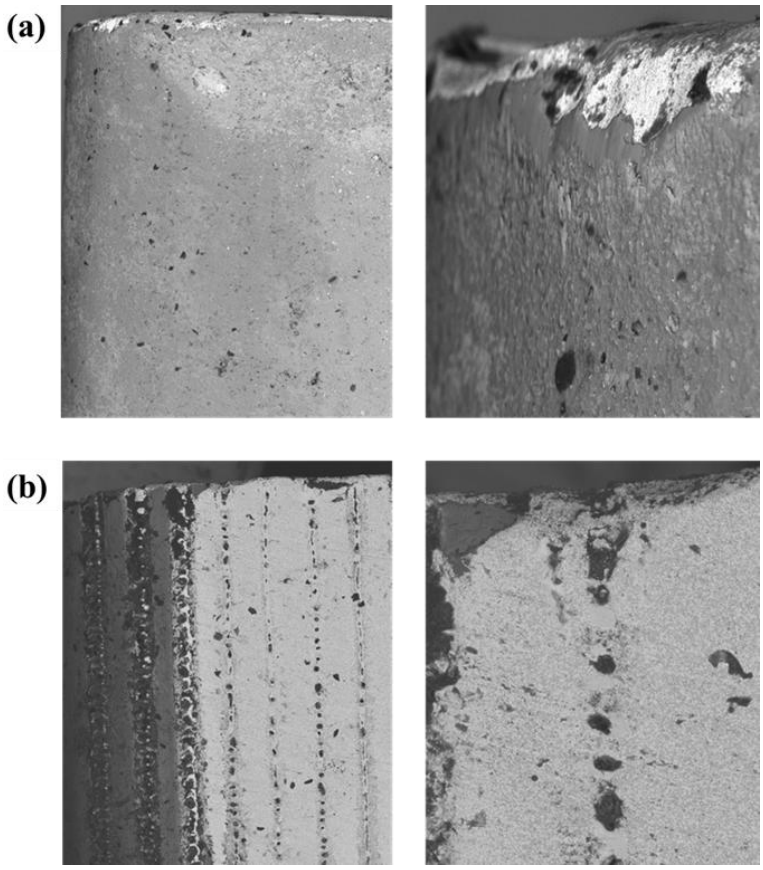

Figure 10: SEM of the conventional and textured tool insert at 500 rpm, depth of cut is 0.16 mm and feed rate is 0.8 mm/rev

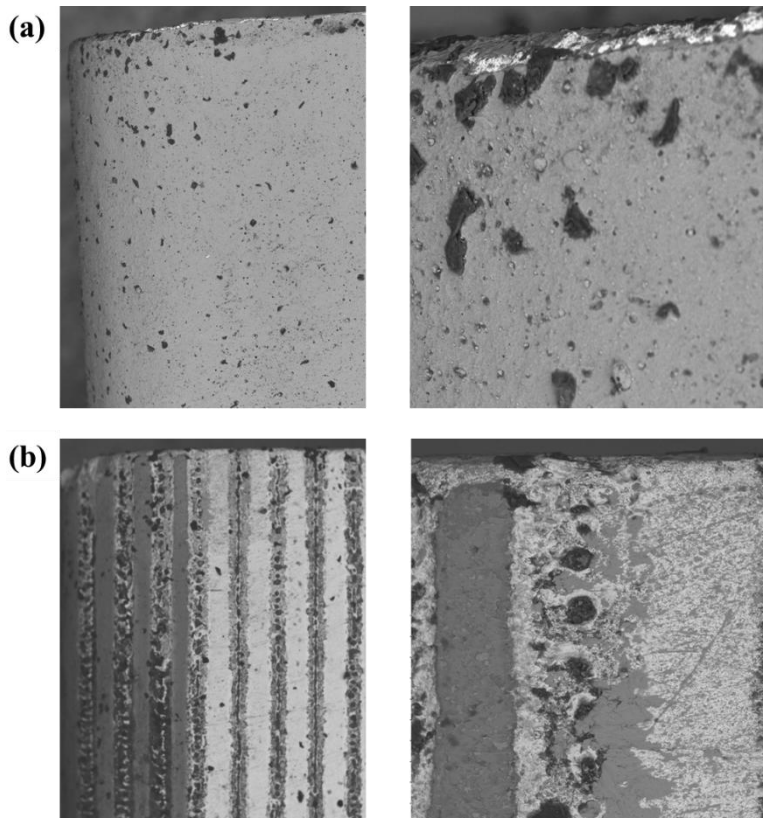

Figure 11: SEM of the conventional and textured tool insert at 775 rpm, depth of cut is 0.16 mm and feed rate is 1.6 mm/rev

From these SEM observations, it is evident that the primary wear mechanisms in the conventional insert are adhesion, abrasion, and material smearing, which intensify with increasing machining parameters. In the textured insert, these mechanisms are significantly mitigated because the micro-grooves reduce real contact area, interrupt adhesive junction formation, trap wear debris, and distribute stresses more evenly across the flank surface. As a result, the textured insert exhibits milder and more uniform wear patterns compared to the severe localized damage observed in the conventional insert.

3.4. Surface Topography and Surface Finish of the Machined Workpiece

The quality of the machined surface produced by the conventional and scorpion-textured inserts was evaluated using 3D surface profilometry. The surface topography maps obtained for different combinations of spindle speed, feed rate, and depth of cut are presented in Figures 12 to 16. These figures provide a direct visual and quantitative comparison of the surface characteristics imparted by both inserts under identical machining conditions. The peak-to-valley height variations observed in the maps also indicate the order of magnitude of surface roughness generated at each condition.

Figures 12(a) and 12(b) correspond to the lowest machining parameters (315 rpm, 0.12 mm depth of cut, 0.4 mm/rev feed). At this condition, both conventional and textured inserts produce relatively smooth surfaces with minor and regular feed marks. The peak-to-valley height variation is small, typically in the range of 3–5 μm. The frictional interactions at the flank face are comparatively low,

resulting in stable cutting for both tools. Consequently, the difference in surface finish between the two inserts is minimal. This indicates that at low loads and speeds, the benefit of texturing is less pronounced because frictional effects are not dominant.

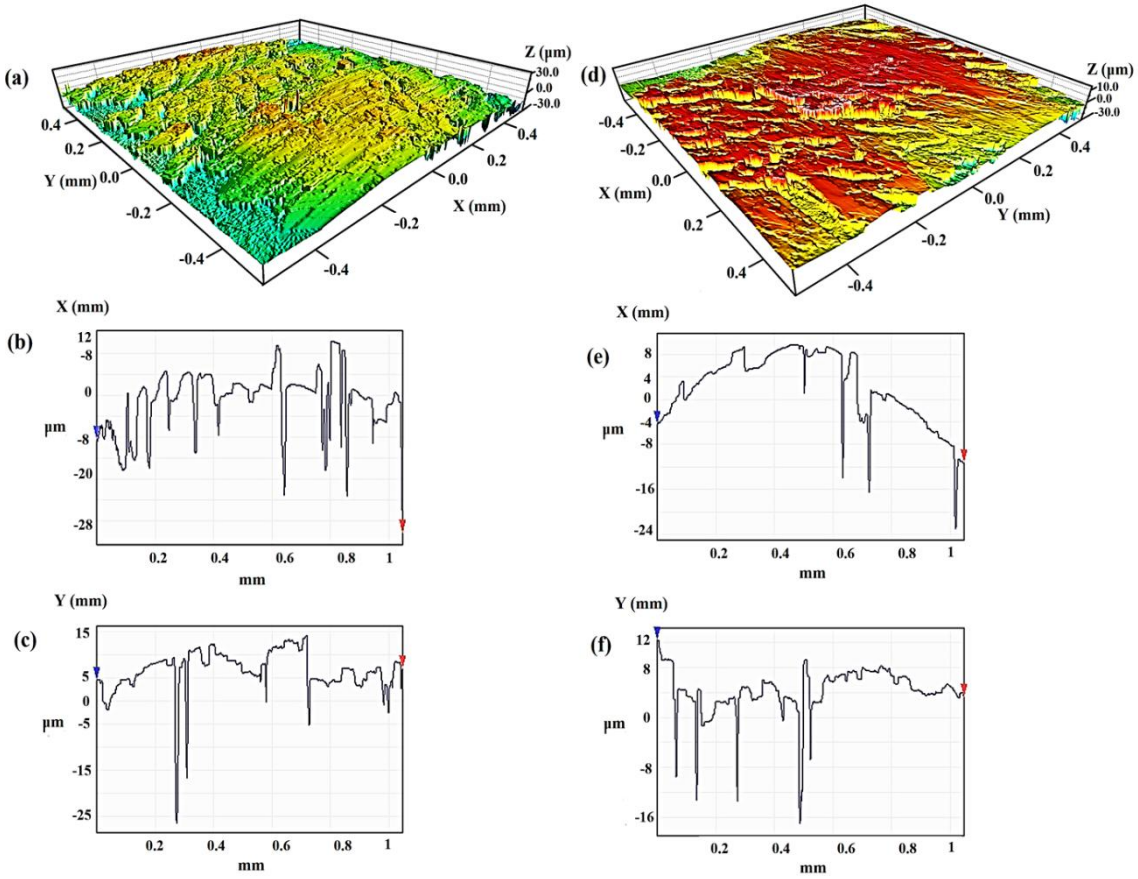

(a)

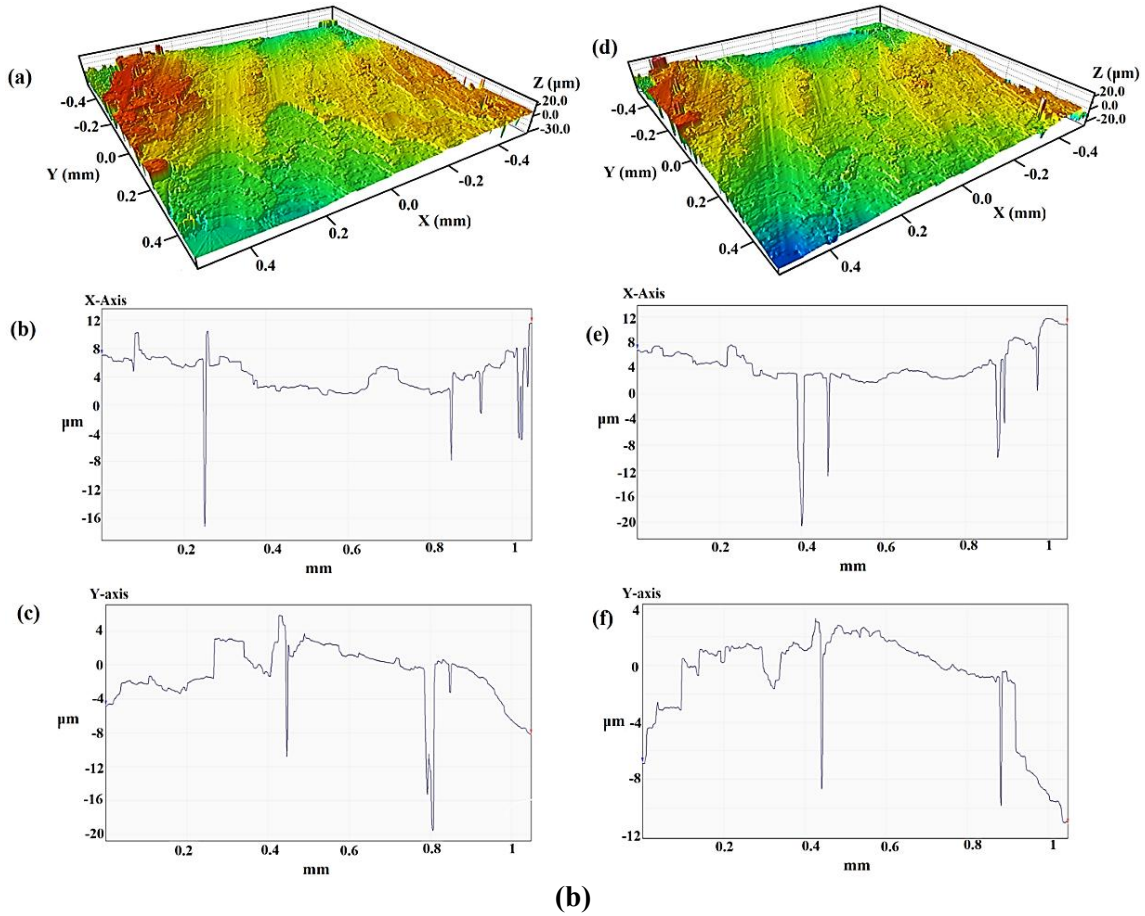

(b)

Figure 12: Surface roughness of (a) conventional and (b) textured tool insert at 315 rpm, depth of cut is 0.12 mm and feed rate is 0.4 mm/rev

Figures 13(a) and 13(b) show the surface topography at increased spindle speed (775 rpm) and feed rate 1.6 mm/rev. The surface produced by the conventional insert exhibits irregular peaks and valleys, micro-tearing, and disturbed feed marks, with height variations increasing to approximately 8–12 µm. This roughness arises due to built-up edge formation and fluctuating adhesion at the flank surface, which introduces micro-vibrations and unstable material removal. In contrast, the textured insert produces a more uniform surface with smoother ridges and reduced height variation of about 5–7 µm. The reduction in real contact area and flank friction stabilizes the cutting process and suppresses vibration.

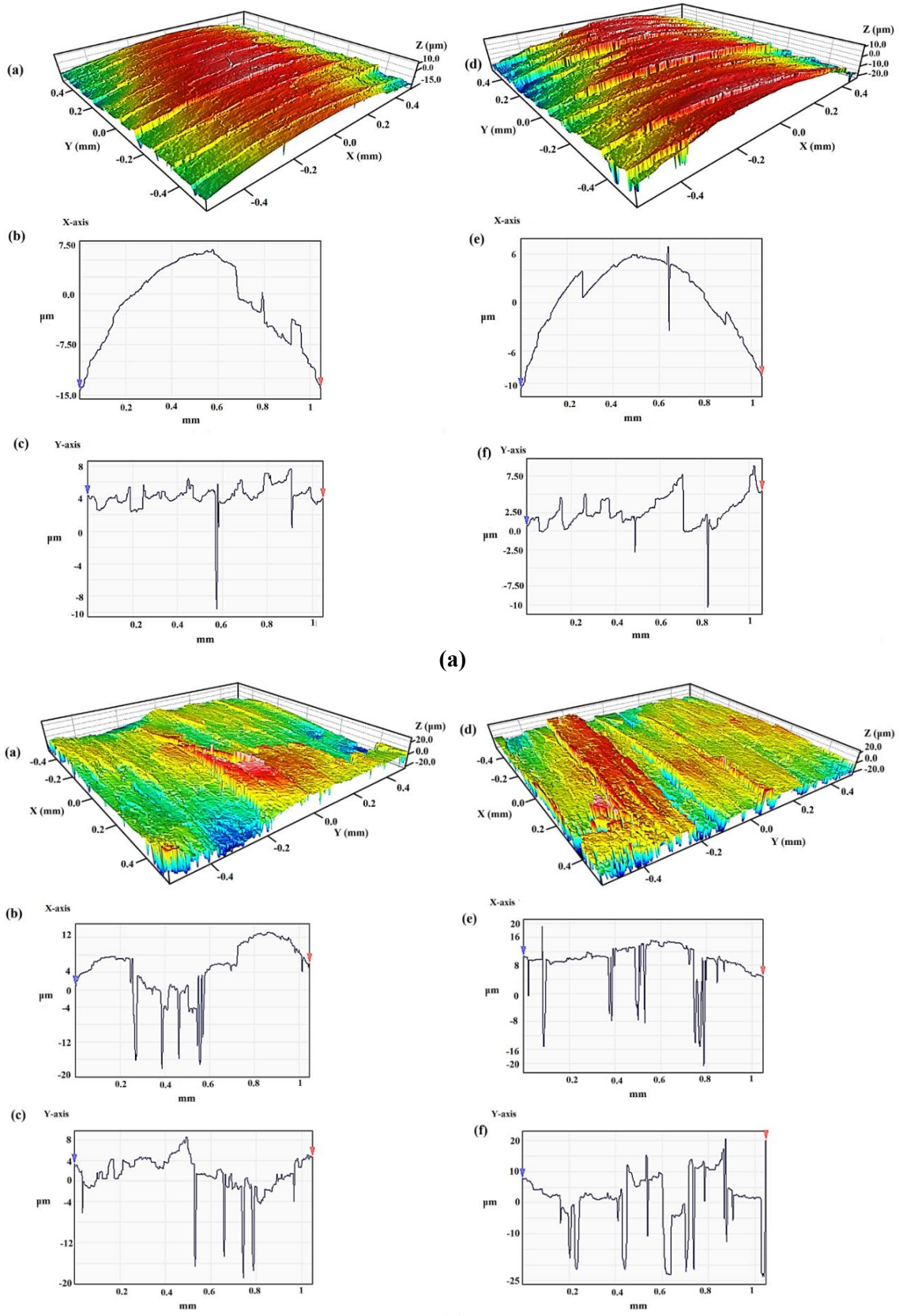

Figure 13: Surface roughness of (a) conventional and (b) textured tool insert at 775 rpm, depth of cut is 0.12 mm and feed rate is 1.6 mm/rev

Figures 14(a) and 14(b) represent moderate combinations of spindle speed 500 rpm, feed rate (0.08 mm/rev) and depth of cut (0.16 mm). The conventional insert surface displays noticeable waviness and irregularity, with peak-to-valley variation reaching nearly 12–15 µm. This is caused by adhesive interaction, higher contact pressure, and tool chatter. The textured insert, however, maintains a consistent surface profile with reduced variation of approximately 7–9 µm. The grooves on the flank surface redistribute contact stresses, reduce adhesion, and ensure steady sliding contact, leading to improved surface integrity.

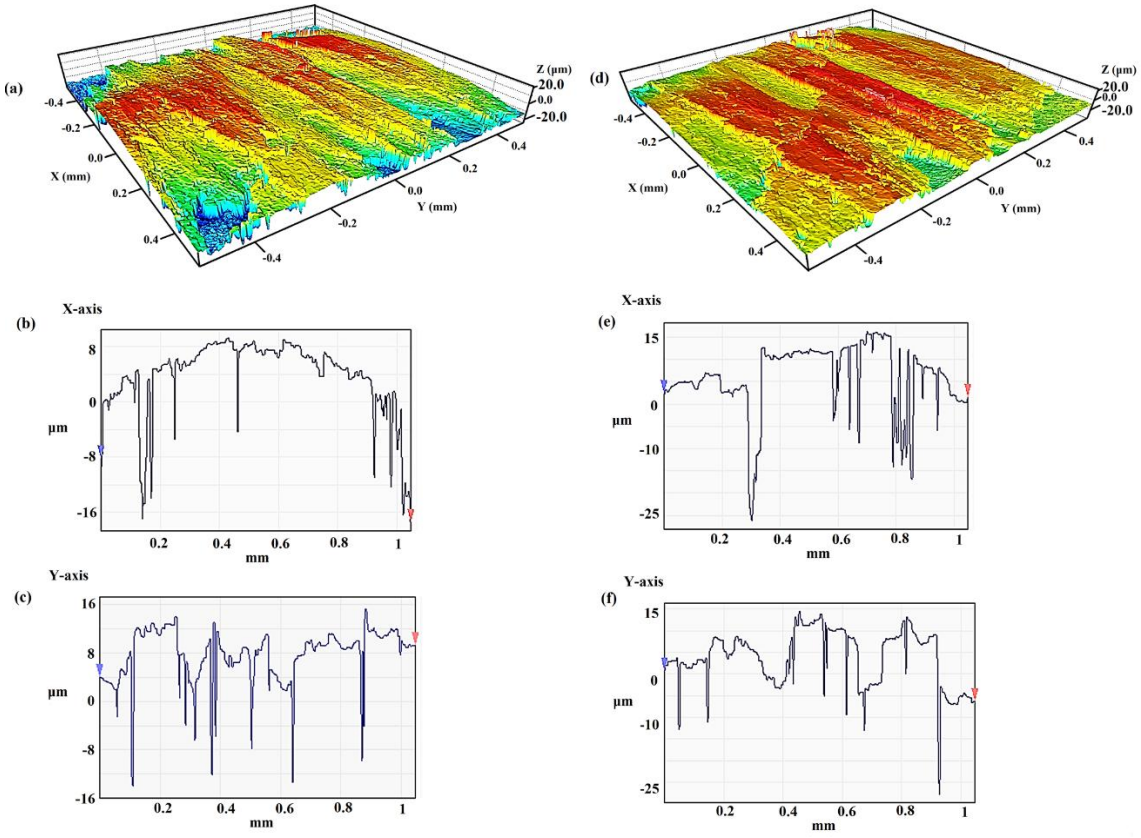

(a)

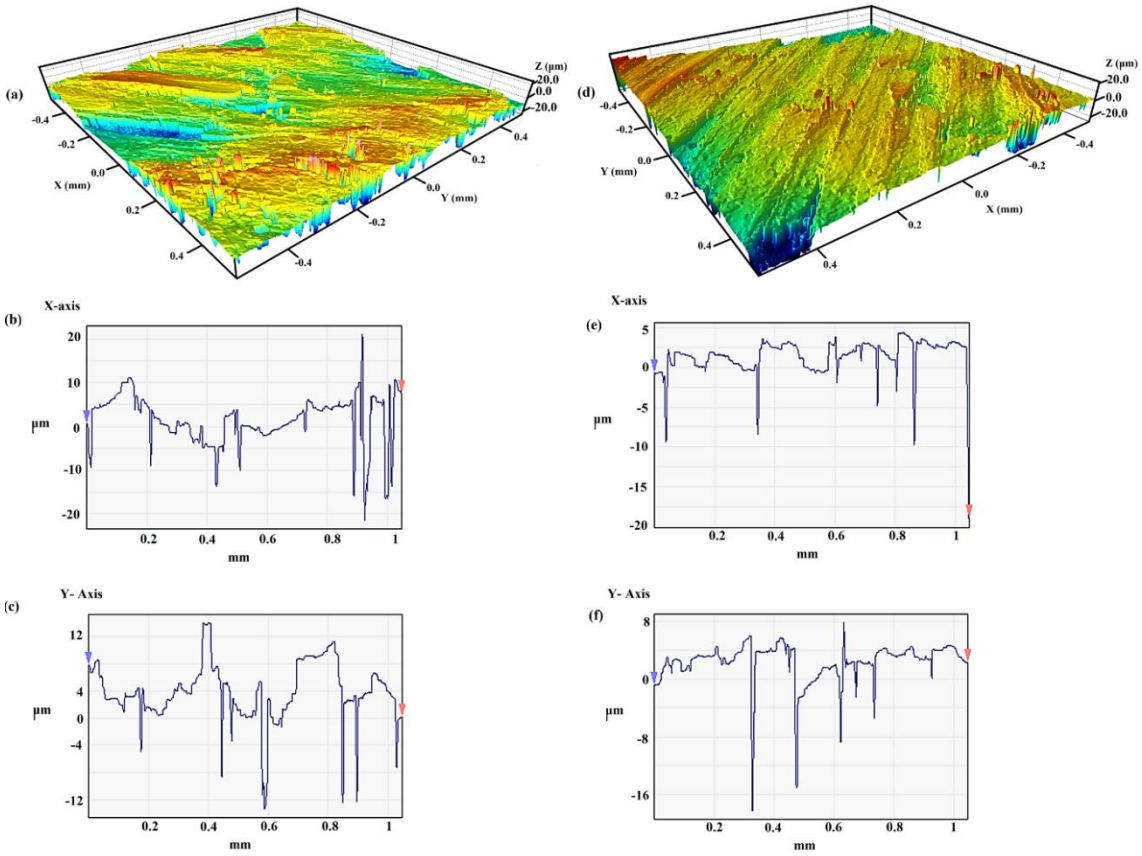

(b)

Figure 14: Surface roughness of (a) conventional and (b) textured tool insert at 500 rpm, depth of cut is 0.16 mm and feed rate is 0.8 mm/rev

Figures 15(a) and 15(b) correspond to higher feed rates (1.6 mm/rev). Under these conditions, the conventional insert produces a rougher surface with deeper grooves and uneven material removal, with height differences approaching 15–20 µm. The increased feed intensifies contact pressure and adhesion at the flank face, and trapped debris ploughs the surface. In the textured insert, debris particles are trapped within the grooves, preventing third-body abrasion. As a result, the surface variation remains comparatively lower, typically around 8–10 µm.

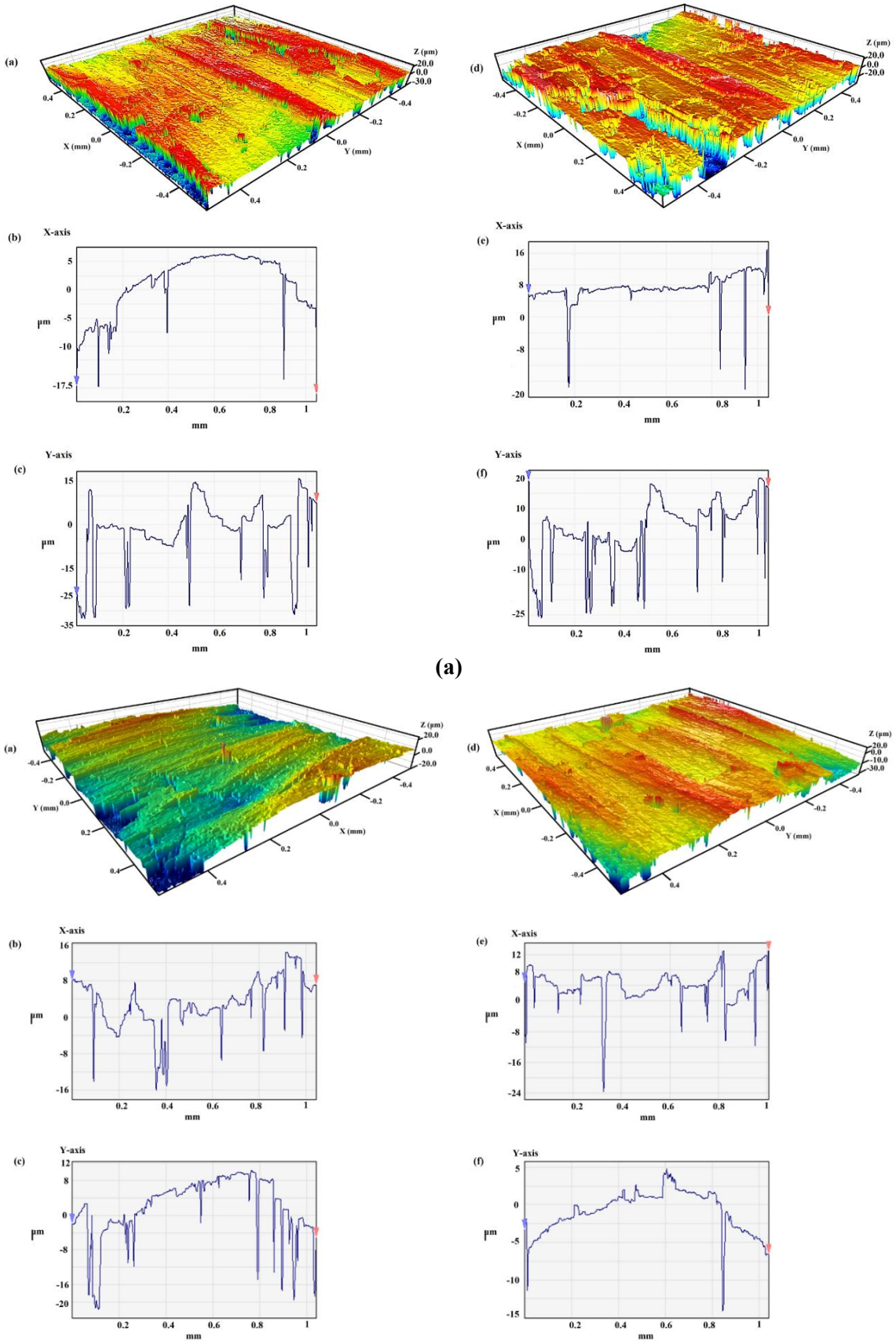

Figure 15: Surface roughness of (a) conventional and (b) textured tool insert at 775 rpm, depth of cut is 0.16 mm and feed rate is 1.6 mm/rev

Figures 16(a) and 16(b) show the surface finish at the highest combination of spindle speed, feed rate, and depth of cut (500 rpm, 0.20 mm DOC, 0.8 mm/rev feed). The difference between the two inserts becomes most evident here. The surface produced by the conventional insert is highly irregular with pronounced peaks and valleys reaching 20–25 µm, indicating unstable cutting conditions, severe adhesion, and vibration at the flank interface. In contrast, the textured insert yields a significantly more uniform and smoother surface with variations limited to approximately 10–12 µm even under these extreme parameters.

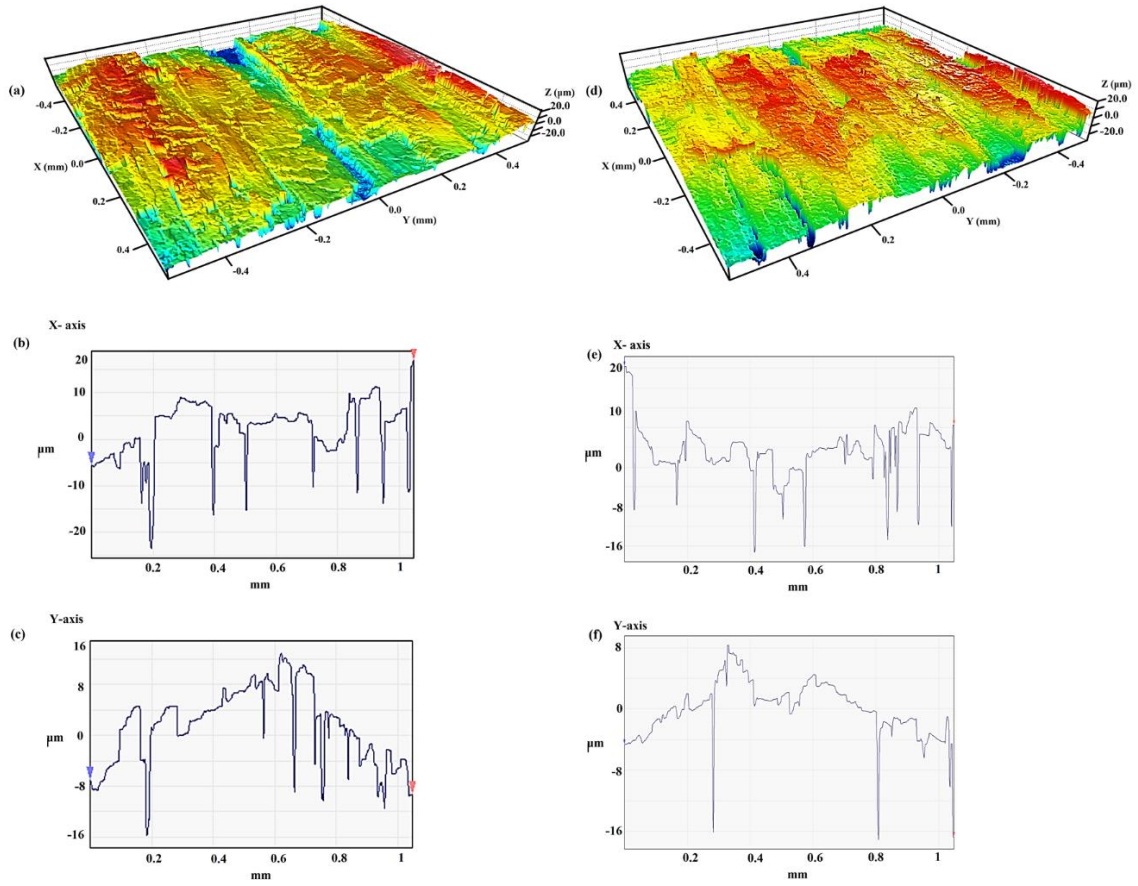

(a)

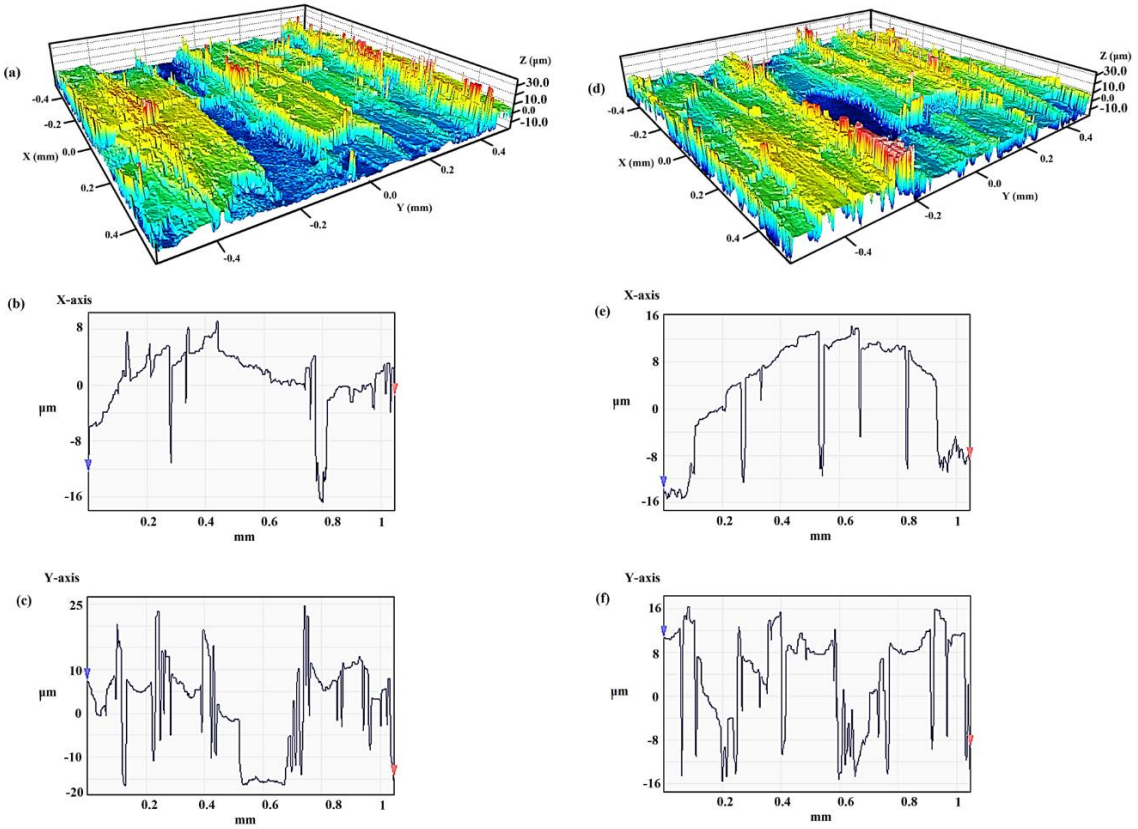

(b)

Figure 16: Surface roughness of (a) conventional and (b) textured tool insert at 500 rpm, depth of cut is 0.20 mm and feed rate is 0.8 mm/rev

This behavior closely reflects the functional principle observed in scorpion cuticle morphology, where ridge–groove surface features regulate interfacial contact and suppress resistance during motion. Similarly, the biomimetic grooves on the flank surface minimize adhesion and friction-induced disturbances, leading to improved surface integrity of the machined workpiece. The enhancement in surface finish is therefore interpreted through tribological evidence obtained from temperature rise, wear characteristics, and surface topography, rather than any direct force measurement. The improved surface integrity is also consistent with the increased tool life of the textured insert, as reduced flank wear ensures stable tool geometry during machining.

4. Conclusions

A comparative experimental investigation was carried out to assess how scorpion-inspired micro-grooves on the flank surface of tungsten carbide inserts influence tribological and thermal behavior during dry turning of C-20 steel. Uniform grooves with 0.2 mm spacing were fabricated using a fiber laser system, and tool performance was evaluated through measurements of tool-tip temperature rise, wear by weight loss, SEM wear morphology, estimated tool life from wear data, and 3D surface

profilometry across a broad range of spindle speeds, feed rates, and depths of cut. The study leads to the following conclusions:

- Textured inserts exhibited up to 50% lower wear, corresponding to nearly 100% improvement in effective tool life due to slower wear progression at the flank interface.
- The tool-tip temperature rise was reduced by 1–6 °C for textured inserts, demonstrating that the performance improvement is primarily due to reduced frictional heat generation rather than enhanced cooling.
- SEM observations confirmed severe adhesion, material smearing, and abrasion on conventional inserts, while textured inserts showed uniform and controlled wear patterns with clearly preserved groove geometry.
- Surface profilometry revealed significantly improved surface finish with textured inserts, especially at higher spindle speeds and feed rates where frictional effects dominate the cutting process.
- These mechanisms directly parallel the drag-reduction and contact-regulation strategies observed in scorpion cuticle morphology.

Overall, the results demonstrate that scorpion-inspired flank biomimetic surface texturing provides an effective biomimetic strategy to reduce friction, wear, and thermal loading during dry machining. The increase in effective tool life further demonstrates the practical engineering benefit of translating scorpion-inspired surface architecture to cutting tool design. This approach enhances tool life and surface quality while promoting energy-efficient and sustainable machining without the need for external lubrication.

Acknowledgements

The author gratefully acknowledges the support of colleagues and laboratory staff who assisted in conducting the turning experiments, SEM imaging, and surface profilometry measurements. The author also acknowledges the use of ChatGPT for language refinement in preparing the manuscript. The scientific content, experimental design, data acquisition, analysis, and interpretations presented in this work are solely those of the author.

Conflict of Interest

The author declares that there is no conflict of interest regarding the publication of this manuscript.

Data Availability Statement

The experimental data supporting the findings of this study are available from the corresponding author upon reasonable request.

Ethics Statement

This study does not involve human participants, animals, or biological specimens. Therefore, ethical approval and informed consent were not required.

References

[1] W. Grzesik, Influence of tool wear on surface roughness in hard turning using differently shaped ceramic tools, Wear 265 (2008) 327–335. https://doi.org/10.1016/j.wear.2007.11.001.

[2] T. Sugihara, T. Enomoto, Performance of cutting tools with dimple textured surfaces: A comparative study of different texture patterns, Precis. Eng. 49 (2017) 52–60. https://doi.org/10.1016/j.precisioneng.2017.01.009.

[3] T. Sugihara, P. Singh, T. Enomoto, Development of novel cutting tools with dimple textured surfaces for dry machining of aluminum alloys, in: Procedia Manuf., Elsevier B.V., 2017: pp. 111–117. https://doi.org/10.1016/j.promfg.2017.11.013.

[4] W. Xu, C. Li, Y. Zhang, Comparative Analysis of Tool Wear and Workpiece Surface Finish During Turning of SS-316 under MQL Vs Dry conditions, IOP Conf. Ser. Mater. Sci. Eng. 1334 (2025) 012020. https://doi.org/10.1088/1757-899x/1334/1/012020.

[5] M.A. El Hakim, M.D. Abad, M.M. Abdelhameed, M.A. Shalaby, S.C. Veldhuis, Wear behavior of some cutting tool materials in hard turning of HSS, Tribol. Int. 44 (2011) 1174–1181. https://doi.org/10.1016/j.triboint.2011.05.018.

[6] K. Bouacha, M.A. Yallese, S. Khamel, S. Belhadi, Analysis and optimization of hard turning operation using cubic boron nitride tool, Int. J. Refract. Metals Hard Mater. 45 (2014) 160–178. https://doi.org/10.1016/j.ijrmhm.2014.04.014.

[7] Y. Xing, J. Deng, X. Wang, K. Ehmann, J. Cao, Experimental assessment of laser textured cutting tools in dry cutting of aluminum alloys, Journal of Manufacturing Science and Engineering, Transactions of the ASME 138 (2016). https://doi.org/10.1115/1.4032263.

[8] J. Ma, N.H. Duong, S. Chang, Y. Lian, J. Deng, S. Lei, Assessment of microgrooved cutting tool in dry machining of AISI 1045 steel, Journal of Manufacturing Science and Engineering, Transactions of the ASME 137 (2015). https://doi.org/10.1115/1.4029565.

[9] D. Jianxin, W. Ze, L. Yunsong, Q. Ting, C. Jie, Performance of carbide tools with textured rake-face filled with solid lubricants in dry cutting processes, Int. J. Refract. Metals Hard Mater. 30 (2012) 164–172. https://doi.org/10.1016/j.ijrmhm.2011.08.002.

[10] M. Mazzonetto, M.R. Saffioti, M. Sanguedolce, V. Siciliani, R. Pelaccia, G. Rotella, D. Umbrello, L. Orazi, L. Filice, Development of micro-texture patterns of cemented carbide cutting tools to improve cutting performance, Procedia CIRP 124 (2024) 608–611. https://doi.org/10.1016/j.procir.2024.08.184.

[11] S.N. Grigoriev, T.N. Soe, K. Hamdy, Y. Pristinskiy, A. Malakhinsky, I. Makhadilov, V. Romanov, E. Kuznetsova, P. Podrabinnik, A.Y. Kurmysheva, A. Smirnov, N.W. Solís Pinargote,

The Influence of Surface Texturing of Ceramic and Superhard Cutting Tools on the Machining Process—A Review, Materials 15 (2022) 6945. https://doi.org/10.3390/ma15196945.

[12] J.M. Arroyo, A.E. Diniz, M.S.F. de Lima, Wear performance of laser precoating treated cemented carbide milling tools, Wear 268 (2010) 1329–1336. https://doi.org/10.1016/j.wear.2010.02.009.

[13] J. Garcia-Fernandez, J. Salguero, M. Batista, J.M. Vazquez-Martinez, I. Del Sol, Laser Surface Texturing of Cutting Tools for Improving the Machining of Ti6Al4V: A Review, Metals 2024, Vol. 14, 14 (2024). https://doi.org/10.3390/met14121422.

[14] S.K. Sharma, H.S. Grewal, Tribological Behavior of Bioinspired Surfaces, Biomimetics 8 (2023) 62. https://doi.org/10.3390/biomimetics8010062.

[15] A. Roushan, Chetan, Influence of laser parameters on the machining performance of textured cutting tools, Opt. Laser Technol. 165 (2023) 109569. https://doi.org/10.1016/j.optlastec.2023.109569.

[16] S. Wu, D. Wang, J. Yin, Research on the Influence of Tool Surface Texture on Cutting Performance Based on Finite Element Method, Micromachines (Basel). 13 (2022) 1091. https://doi.org/10.3390/mi13071091.

[17] A. Çalik, Effect of Dimensions in Laser Surface Texturing on Cutting Tools, Mechanika 31 (2025) 428–434. https://doi.org/10.5755/j02.mech.35761.

[18] N. Maani, V.S. Rayz, M. Nosonovsky, Biomimetic approaches for green tribology: from the lotus effect to blood flow control, Surf. Topogr. 3 (2015) 034001. https://doi.org/10.1088/2051-672X/3/3/034001.

[19] D.K. Pandey, H.C. Lim, Green machining with bionic textured tungsten carbide inserts, in: Proceedings of the 20th Cross Straits Symposium on Energy and Environmental Science and Technology, Busan, 2018: p. 2.

[20] Y. Lu, M. Hua, Z. Liu, The biomimetic shark skin optimization design method for improving lubrication effect of engineering surface, J. Tribol. 136 (2014). https://doi.org/10.1115/1.4026972.

[21] Z. Han, H. Feng, W. Yin, S. Niu, J. Zhang, D. Chen, An Efficient Bionic Anti-Erosion Functional Surface Inspired by Desert Scorpion Carapace, Tribology Transactions 58 (2015) 357–364. https://doi.org/10.1080/10402004.2014.971996.

[22] N. Rogkas, G. Adamopoulos, D. Skondras-Giousios, V. Spitas, Design, analysis and comparative study of bio-inspired surface texturing for enhanced drag reduction in rotating hydrodynamic lubrication regimes, Tribol. Int. 210 (2025) 110750. https://doi.org/10.1016/j.triboint.2025.110750.

[23] W. Huang, X. Wang, Biomimetic design of elastomer surface pattern for friction control under wet conditions, Bioinspir. Biomim. 8 (2013) 046001. https://doi.org/10.1088/1748-3182/8/4/046001.

[24] J. Nagpal, R. Rana, R. Lal, R. Muttanna Singari, H. Kumar, A brief review on various effects of surface texturing using lasers on the tool inserts, Mater. Today Proc. 56 (2022) 3803–3812. https://doi.org/10.1016/j.matpr.2022.01.272.

[25] M.G. Faga, P.C. Priarone, M. Robiglio, L. Settineri, V. Tebaldo, Technological and sustainability implications of dry, near-dry, and wet turning of Ti-6Al-4V alloy, International Journal of Precision Engineering and Manufacturing - Green Technology 4 (2017) 129–139. https://doi.org/10.1007/s40684-017-0016-z.

[26] P.S. Sreejith, B.K.A. Ngoi, Dry machining: Machining of the future, J. Mater. Process. Technol. 101 (2000) 287–291. https://doi.org/10.1016/S0924-0136(00)00445-3.

[27] W. He, Y. Guo, W. Ming, Y. Zhang, L. Duan, J. Du, Development of several green machining technologies in machinery manufacturing and their implementation perspectives, Proc. Inst.

Mech. Eng. C J. Mech. Eng. Sci. 239 (2025) 9282–9305. https://doi.org/10.1177/09544062251359435.

[28] R. Singh, M. Singh, R. Singh, Impact of texture cutting tools on sustainable machining methods: a review, International Journal on Interactive Design and Manufacturing (IJIDeM) 2024 19:5 19 (2024) 3121–3137. https://doi.org/10.1007/s12008-024-01957-1.